LA-UR-19-26211
Approved for public release; distribution is unlimited.

| | |
|---|---|
| Title: | Optical properties of BaFCl:Eu2+ scintillating composites for X-ray imaging screens |
| Author(s): | Richards, Cameron Gregory |
| Intended for: | Report |
| Issued: | 2019-07-02 |

# Optical properties of BaFCl:$Eu^{2+}$ scintillating composites for X-ray imaging screens

**CAMERON G. RICHARDS,**[1,2,*]

[1]*Graduate Research Intern, MST-7 Engineered Materials, Los Alamos National Laboratory, Bikini Atoll Rd., SM 30, Los Alamos, NM 87545, USA*
[2]*Optical Materials and Devices, Masters Industrial Internship Program, 1252 University of Oregon Eugene, OR 97403, USA*
**crichar7@uoregon.edu*

**Abstract:** The development of composite scintillating materials is necessary for the optimization of advanced pixelated X-ray imaging technology. Polycrystalline BaFCl:$Eu^{2+}$ was synthesized via a flux growth technique and its emission properties were characterized through photo-luminescence (PL) spectroscopy and time-correlated single photon counting (TCSPC). PL emission wavelengths were observed at 365 nm, 383 nm, and 430 nm under UV excitation. Composite pastes, consisting of BaFCl:$Eu^{2+}$ powder and NOA1665 UV-curable resin, were fabricated and subsequently analyzed through absorption and radio-luminescence (RL) spectroscopy. An interchange of transmissivity and light production, resulting from differences in the amount of solvent and resin in the composite, was observed in fabricated composites.

## 1. Introduction

### *1.1 Radiography in the medical industry*

Of the plethora of procedures employed in the medical industry for diagnosing and analyzing patients, radiography has proven to be an invaluable tool. Computed tomography (CT) and positron emission tomography (PET), to name two applications, are utilized globally for their ability to non-intrusively provide high-quality visualizations of patient interiors. While these techniques are vital within the medical sector, these processes are not considered risk-free. Cell degradation and cancer, resulting from extended ionizing radiation exposure, constrains the duration patients may be exposed to ionizing radiation. Due to this fact, minimizing radiation exposure time while maximizing image quality is critical for the safety of the patient and for subsequent analysis.

Current CT technology typically relies on image generation through a two-step process involving a composite storage phosphor plate. The phosphor plate acts as a wavelength shifter, converting X-rays to visible light through electron-hole recombination engendered by the irradiation event. When released, the visible photons must be able to efficiently travel through the material to be picked up by a photo-detector (PD) or photo-multiplier tube (PMT). Since current composite phosphors can be highly opaque to visible light, only a small fraction of the visible photons may actually reach the detector, resulting in a loss of information. One solution to this problem is through the use of a composite material containing the phosphor and an optical binding agent with matching refractive indices.

### *1.2 Composite scintillator*

Similar to the design envisioned by *Cusano et al.*, a scintillator paired with an optical binding agent of like refractive index can significantly improve light transport through the composite material. By matching the refractive indices, the amount of optical loss due to scattering from Fresnel reflections may be reduced. When coupled to a photodetector, the improvement in light transport within the composite can enhance the detection response, effectively reducing the corresponding dose and time required to build an image with statistical confidence. This is highly advantageous for radiological purposes, particularly for computed tomography. In this paper, we focus our attention on Eu(II)-doped BaFCl as the scintillator of choice.

### *1.3 BaFCl:$Eu^{2+}$ scintillator system*

The luminescent properties of the barium fluorohalides ($BaFCl:Eu^{2+}$, $BaFBr:Eu^{2+}$) have been discussed and characterized under a variety of conditions, providing a desirable level of technical maturity [1, 2, 4, 5, 7, 8, 10-12, 14-18]. It has been shown that $BaFCl:Eu^{2+}$ exhibits peak emissions under UV- and X-irradiation near 365 nm, 385 nm, and 430 nm on numerous occasions [1, 2, 5, 7, 12, 15-18]. The emissions at 365 nm and 385 nm can be attributed to the $^6P_{7/2} \rightarrow {}^8S_{7/2}$ and $4f^65d^1 \rightarrow {}^8S_{7/2}$ electronic transitions of $Eu^{2+}$ ions. The emission at 430 nm has also been reported to be due to the $4f^7 \rightarrow 4f^65d^1$ transition of the $Eu^{2+}$ ion, and has been shown to be present with the $Ba_{12}F_{19}Cl_5$ phase [10]. Additionally, an interplay relationship may exist between the emissions at 385 nm and 430 nm when the secondary phase is present; the increase in emission intensity of one peak may result in a decrease of the other. As discussed in the previous paper, creation of the secondary phase can be controlled during synthesis by adjusting the dwelling time. The photo-luminescence (PL) has also been reported to have decay lifetimes in the µs regime [7, 16]. These attributes suggest the scintillator is an ideal candidate for use with radiometric detection applications.

Here, we aim to pair $BaFCl:Eu^{2+}$ polycrystalline powder with commercially available optical adhesive from Norland Products. Emphasis is placed on understanding the interactions between the fundamental components of the composite during formation. To elucidate compositional trends within the composite system, the amount of $BaFCl:Eu^{2+}$ was held constant for each mixture while different quantities of IPA and NOA1665 were explored. The ideal complex of scintillator, resin, and solvent will produce a composite with well-balanced transmissivity and scintillation properties.

Since the refractive index of $BaFCl:Eu^{2+}$ is approximately 1.68 near 385 nm, given by the dispersion curve in figure 1, a mixture of NOA1665 (n = 1.665) and NOA170 (n = 1.70) can create a curable binder with the index-matched condition. Following the optimization studies done here, future work will be conducted to achieve index-matching.

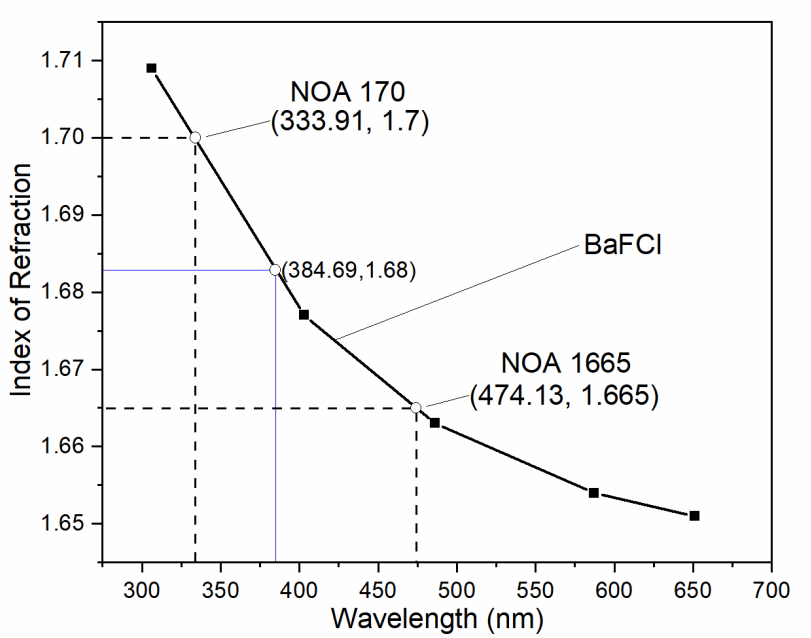


*Fig. 1. Dispersion curve of BaFCl:$Eu^{2+}$ over the visible spectrum. Index values for commercially available UV-curable resins are included for reference. At a wavelength of 385 nm, corresponding to a peak emission of the $Eu^{2+}$ ion, the index lies at 1.68. Mixing the two resins can produce a new resin with a matching refractive index.*

## 2. Experimental

### *2.1 BaFCl:$Eu^{2+}$ synthesis and characterization*

Multiple batches of BaFCl:$Eu^{2+}$ powder were synthesized via a flux growth technique with $BaF_2$(s), $BaCl_2$(s), and $EuF_2$(s) reagents. Under inert atmosphere, the reagents were mixed in a glassy carbon crucible with a 20% mol excess of $BaCl_2$. Each synthesis trial was heated to 1100˚C to form a molten mixture, and allowed to dwell at the process temperature for 4 hours, 12 hours, 2 hours, and 30 minutes, respectively. Crystalline BaFCl:$Eu^{2+}$ is formed upon cooling.

Following synthesis, each yield was lightly crushed and filtered with DI water to remove excess $BaCl_2$. The filtered yields were then annealed at 120˚C for 18 hours under ambient atmosphere to evaporate residual moisture. Yields 2 through 4 were size-separated using a multi-layered sieve with mesh sizes 75 µm, 53 µm, and 38 µm. PL spectra were acquired for representative samples of each yield, and for each particle size-subset using a Photon Technology Inc. fluorescence spectrometer. Measurements of the PL emission decay characteristics were performed on the BaFCl:$Eu^{2+}$ powder using a Horiba DeltaPro time-correlated single photon counting (TCSPC) spectrofluorometer with a 20 MHz pulsed excitation source at 335 nm. Analysis and fitting of the lifetime measurements were done on the Horiba DAS6 software.

### *2.2 Composite paste development*

Norland Optical Adhesive 1665 (n = 1.665) was added to cups containing approximately 0.5 g of BaFCl:$Eu^{2+}$ powder from Trial 3. Isopropyl alcohol was included to act as a cooling agent during the mixing process. To form a composite paste, the constituents were mixed in a Thinky Planetary Vacuum Mixer by the procedure outlined in Table 1. Once the mixing cycle was complete, the paste was cast into cylinders approximately Ø7.92 mm x 1.7 mm thick and cured with a 365 nm UV lamp.

*Table 1. Thinky Mixer cycle for composite paste development.*

| Step | Speed (rpm) | Vacuum (kPa) | Duration (min.sec) |
|---|---|---|---|
| 1 | 2000 | Off | 0.30 |
| 2 | 500 | Off | 2.00 |
| 3 | 2000 | Off | 0.30 |
| 4 | 500 | 0.2 | 2.00 |
| 5 | 2000 | 0.2 | 0.30 |

Absorption spectra were acquired for each composite paste using a Varian, Inc. Cary 5000 UV-VIS spectrophotometer over the range of 200-800 nm. Radio-luminescence (RL) spectra were obtained for the generated composite samples using the Cu-Kα X-ray line (15.4059 nm)

## 3. Results and Discussion

### *3.1 Optical properties of BaFCl:$Eu^{2+}$ powder*

The representative PL spectra obtained from each synthesis trial clearly indicated that the dwelling time affects the luminescence of the powder. Shown in figure 2, the trials with the shorter dwell times (2 hours and 30 min) display substantially greater emission properties than those of the trials with longer dwell times (4 hours and 12 hours). The peaks at 362 nm and 383 nm match well to those found in literature; these transitions can be attributed to electronic transitions of the $Eu^{2+}$ ion. The shoulder at 430 nm in Trial 2 can also be related to a transition of the $Eu^{2+}$ ion, but is strongly correlated to the $Ba_{12}F_{19}Cl_5$ phase in the material. The magnitude of the shift in the primary peak at 383 nm in Trial 2 can be related to the strength of the crystal field effect influencing the $Eu^{2+}$ ions.

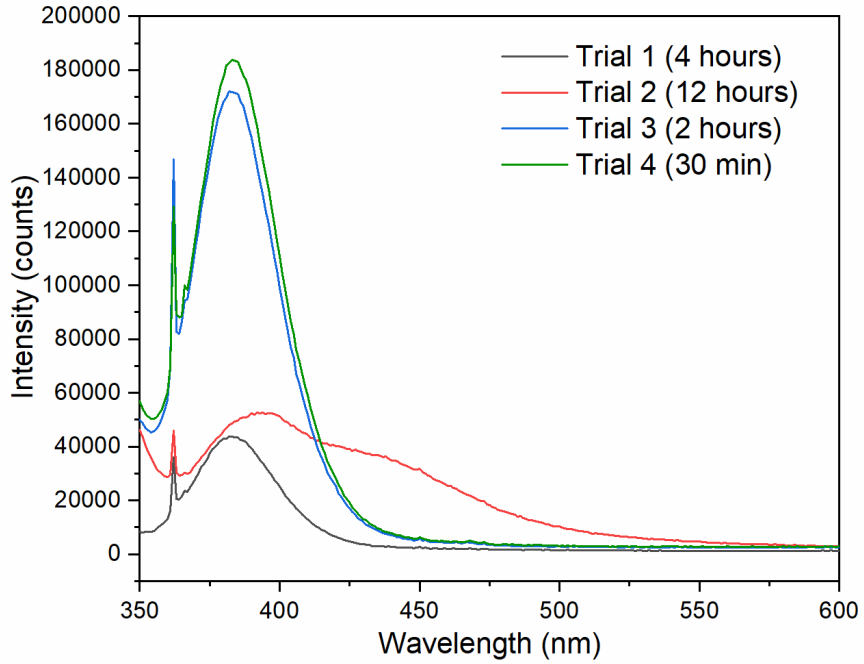


*Fig. 2. Representative PL emissions of the BaFCl:$Eu^{2+}$powder from each Trial. Trials with the shorter dwell times are much brighter.*

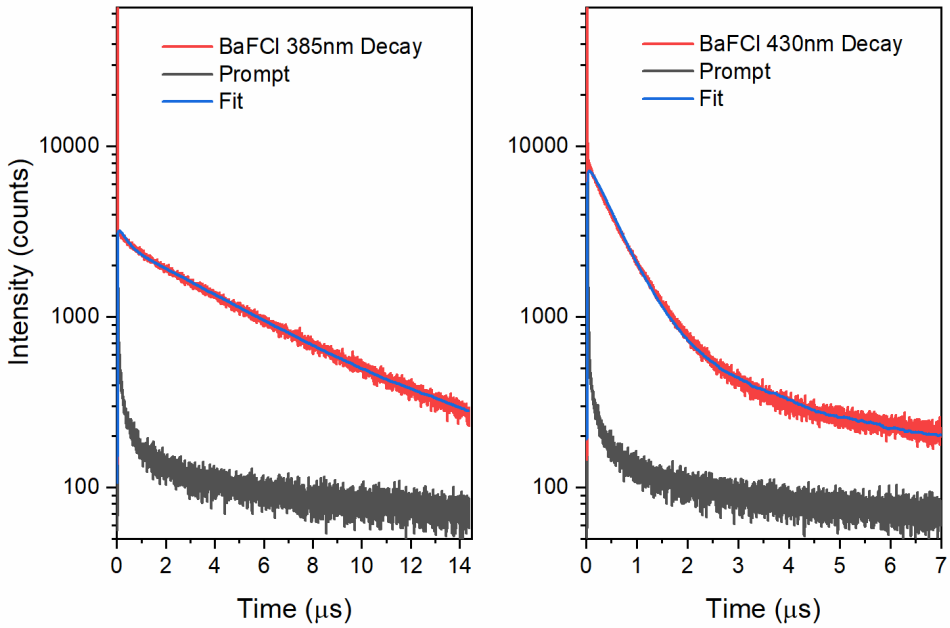


*Fig. 3. Decay lifetimes of PL emissions from BaFCl:$Eu^{2+}$ powder under 335 nm excitation. Left: The lifetime curve for the 385±10 nm emission, fit to a 2nd degree exponential giving a primary time constant of 2.947μs. Right: The lifetime curve for the 430±10 nm emission, fit to a 2nd degree exponential with a primary time constant of 0.4719 μs.*

Lifetime measurements of the large particle subset of Trial 2 can be seen in figure 3. Using band-pass filters to separate the PL emissions of 385 nm and 430 nm, the decays for each emission could be measured. In the figure, the 385 nm BaFCl decay curve was fit to a 2nd degree exponential, resulting in a primary time constant of 2.947 μs; the 430 nm decay was fit to a 2nd degree exponential, yielding a primary time constant of 0.4719 μs. These values are comparable to those found by *Secu et al.*, who measured lifetimes of 3.3 μs and 0.7 μs for the 385 nm emission and 430 nm emission, respectively.

PL analysis was also performed on powder ground by hand to determine if subsequent grinding affected the luminescence of the crystals. By this method, powder from the largest subset of Trial 3 was ground and sieved, producing 0.8 g of powder in the <38 μm subset. As seen in figure 4, the PL emission at 383 nm initially showed no significant difference between the as-synthesized powder and the ground powder. Subsequent repetitions of the process, however, indicated that grinding eventually deteriorated the luminescence. Thus, post-synthesis grinding should be kept to a minimum if the maximum light yield is to be maintained.

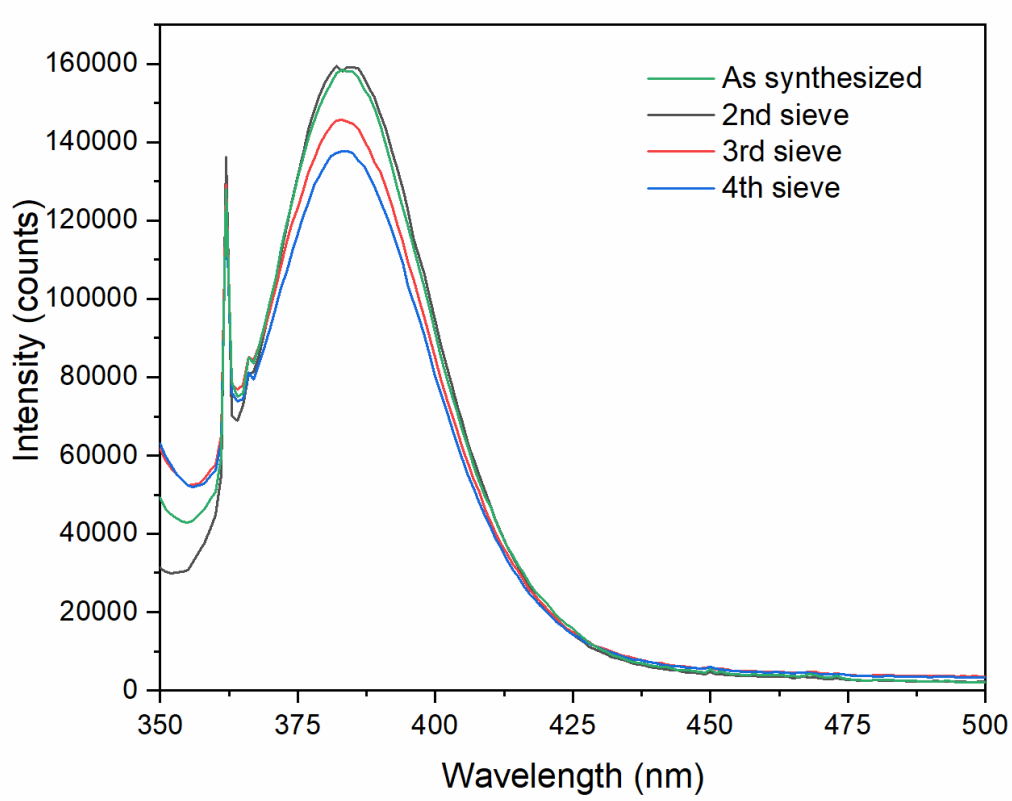


*Fig. 4. PL emissions of BaFCl:$Eu^{2+}$ powder from Trial 3 after post processing. The initial grinding process showed minimal change, but subsequent repetitions indicated deterioration of the luminescence.*

### *3.2 Composite paste development and characterization*

The first paste produced for this study was dark, dry, and unable to be adequately cast into the cylinder form without breaking apart. Since the BaFCl:$Eu^{2+}$ powder is white and the optical adhesive clear, it was suspected that the mixture was contaminated.

To explore this hypothesis, another batch of paste was made with similar parameters, but with careful control over the environmental conditions. Similar undesirable characteristics were observed, suggesting contamination was not likely the root cause of the discoloration or dryness. Comparing the experimental procedure to previous successful instances, the major difference noted was the quantity of solvent used in the mixture. Therefore three new paste mixtures were made with IPA contributions of 50%, 100%, and 150% by weight of material to investigate this parameter. The weight of BaFCl:$Eu^{2+}$ and resin were maintained at approximately 0.5 g and 0.1 g, respectively. After mixing, composites with 50% and 100% ratios produced thicker pastes with a slightly green coloration, while the composite with the 150% ratio was less viscous, appeared white, and was more opaque. These differences in appearance can be seen in figure 5, where the composites are arranged in ascending IPA weight ratios from left to right. It is apparent that the composite with the 50% ratio provided the highest degree of translucency when exposed to UV irradiation.

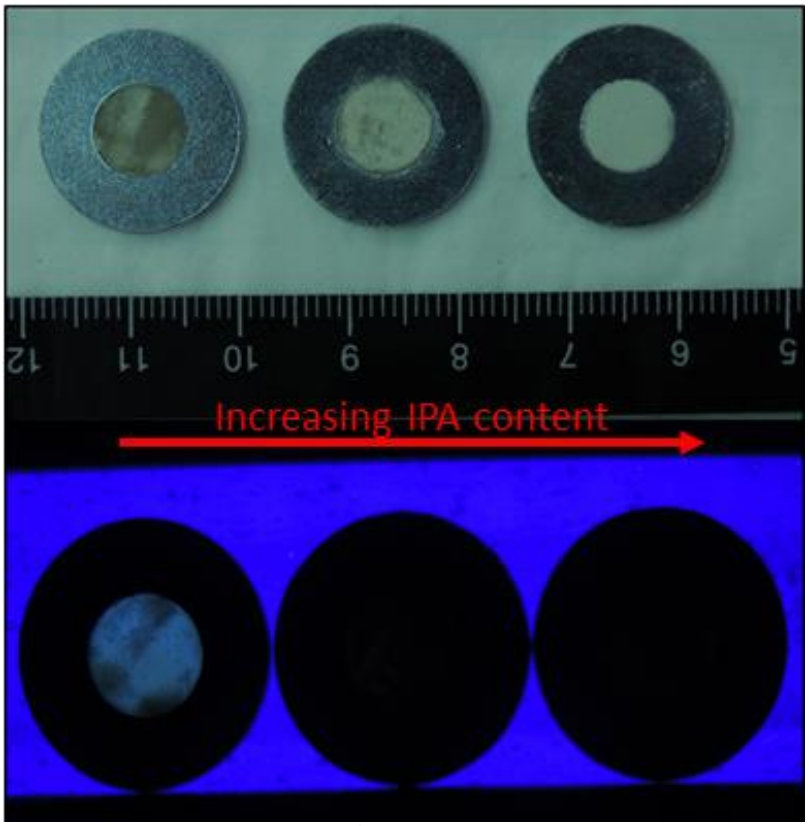


*Fig. 5. Composite pastes casted into the cylindrical forms under ambient (top) and UV (bottom) light exposure. IPA concentration incorporated into the mix increases from left (50%) to right (150%).*

Absorption measurements of the solid composites, shown in figure 6 (left), indicated a correspondence between the amount of solvent used and the absorptivity; composites made with greater amounts of IPA showed increased absorptivity as compared to the batch made with the lowest ratio. The increase in the opacity with larger concentrations of IPA can be due to an abundance of small air voids within the composite. These voids can enhance light scattering, and explain the whiter appearance in conjunction with the greater absorptivity. Also notable in the figure is the absorption peak near 356 nm present in the bottom curve, which is likely due to an absorption artifact of the BaFCl:$Eu^{2+}$ powder or the resin; further research must be done to define its origin.

In the right of figure 6, the RL spectra confirms the materials ability to produce scintillation photons. The primary peaks at 365 nm and 383 nm are related to the same electronic transitions of $Eu^{2+}$ ions seen in the PL spectra. Since the penetration depth of the X-rays is much greater than that of UV radiation, more confidence can be placed in the luminescence within the bulk. Consequently, the depth of interaction also increases the probability of self-absorption events, which may inhibit the visible photons from ever reaching the surface. This inherently leads to an engineering constraint on the maximum possible thickness of the composite that can be used with photo-detectors. Additionally, it is apparent that the material-solvent correlation also affects the RL emission properties. From a radio-luminescence standpoint, the composite with the higher concentration of solvent performed better than the lower concentration composite. Though the brighter emission is desirable, the greater absorptivity associated with it is too strong to be used as a composite mixture for detector applications. Hence from this study, it was determined a 50% solvent-material ratio would be ideal for composite development.

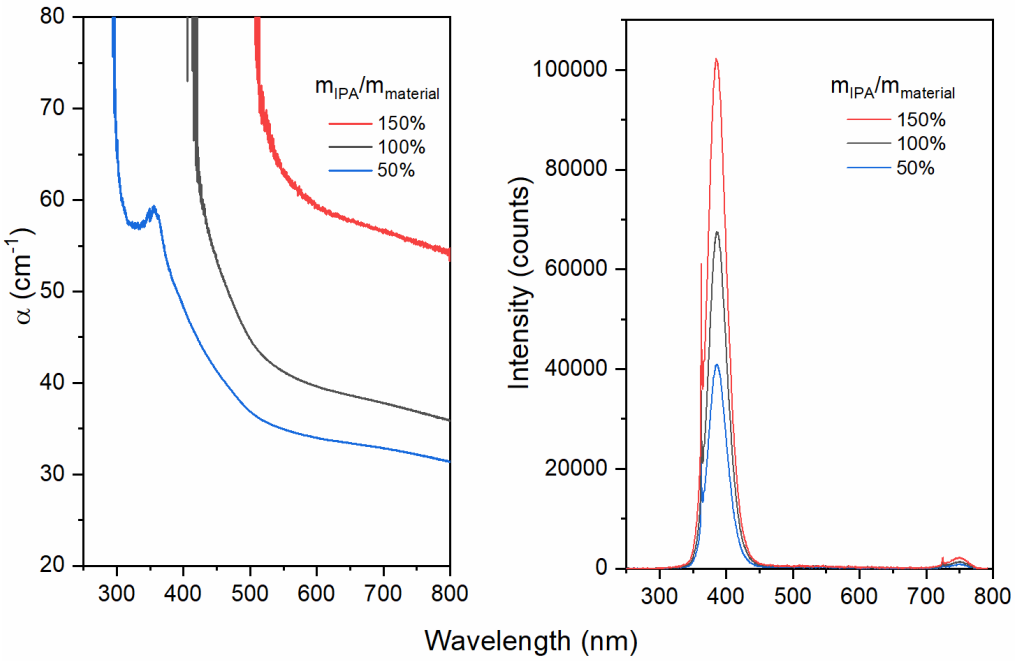


*Fig. 6. Left: Absorption spectra of the composites for varying IPA concentrations. Right: Radio-luminescent spectra of composites with varying IPA concentrations. As can be seen, the amount of IPA used during composite fabrication affects both the absorption and luminescence properties.*

Similar absorption spectra were acquired for composite mixtures of varying BaFCl:$Eu^{2+}$ volume fractions. Using an IPA-material weight ratio of 50% and 0.5 g of BaFCl:$Eu^{2+}$, composites with volume fractions of 50%, 55%, 60%, and 65% were fabricated and tested, the results of which can be seen in figure 7. As expected, reducing the amount of resin relative to the BaFCl:$Eu^{2+}$ diminishes the translucency of the composite. Though translucency is required for visible light propagation, the increased concentration of the scintillator component is ideal for X-ray detection; this element improves the X-ray interaction probability at the cost of translucency, both of which are critical for the technology.

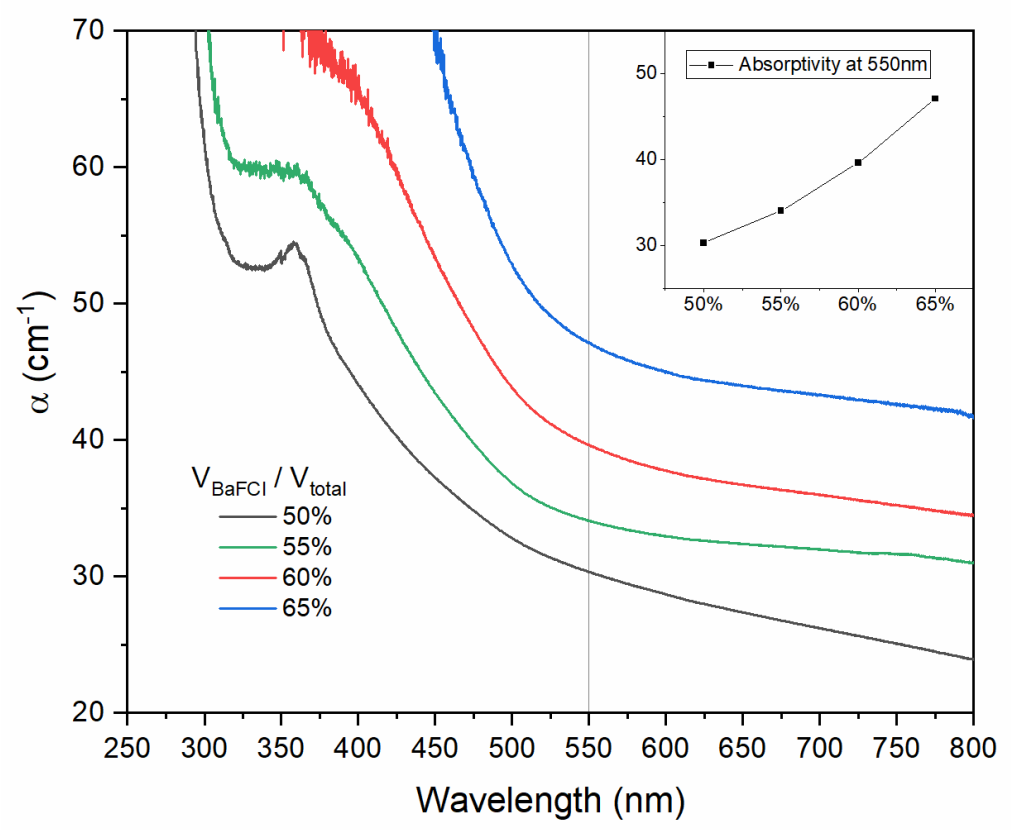


*Fig. 7. Absorption spectra for the BaFCl:$Eu^{2+}$ composite at varying volume fractions. It can be seen that slight increases in the concentration of the scintillator results in substantially higher absorptivity. This relationship can be seen in the inset, where the absorption coefficient at 550 nm is plotted versus the volume fraction.*

## 4. Conclusions

In summary, the synthesis of BaFCl:$Eu^{2+}$ was optimized to produce very bright scintillating powder; it was shown that a reduction in dwelling time during synthesis significantly increases the PL emission properties of the BaFCl:$Eu^{2+}$ crystals. Crushing the BaFCl:$Eu^{2+}$ powder by hand in a mortar and pestle showed little change to the luminescent properties of the scintillator, and is a viable method for producing larger quantities of smaller particles. In addition to the optimization studies of the powder, composite pastes consisting of the BaFCl:$Eu^{2+}$, Norland Optical Adhesive 1665, and isopropyl alcohol were created and characterized by UV-VIS absorption spectroscopy and radio-luminescence. Through characterization, it was determined that the amount of IPA affects both the physical and optical properties of the resulting paste; when greater amounts of IPA is used, the paste is less viscous, less transparent, but brighter under X-irradiation as compared to composites made with less IPA. It was also shown that the amount of resin notably affects the absorptivity of the composite. In this study, it was determined that the optimal conditions for BaFCl:$Eu^{2+}$ scintillating composites consist of a 50% by weight contribution of IPA, and a 50% volume fraction of BaFCl:$Eu^{2+}$.

## Funding

Funding for this project was provided by Los Alamos National Laboratory.

## Acknowledgments

Special thanks to Dr. Brenden Wiggins for mentorship and introduction into the scintillator field.

## References

1. Chen, W., et al. (2005). "X-Ray Storage Luminescence of BaFCl:Eu2+ Single Crystals." The Journal of Physical Chemistry B 109(23): 11505-11511.
2. Chen, W., et al. (1998). "New color centers and photostimulated luminescence of BaFCl:Eu2+." Journal of Physics and Chemistry of Solids 59(1): 49-53.
3. Cusano, D. A., et al. (1983). Index-matched phosphor scintillator structures. United States.
4. Eachus, R. S., et al. (1995). "Oxygen defects in BaFBr and BaFCl." Physical Review B 52(6): 3941-3950.
5. Es-Sakhi, B., et al. (2002). "Photoluminescence of Eu2+ in BaF2-rich fluorohalides and photostimulation after X-ray irradiation." Materials Science and Engineering: B 96(3): 233-239.
6. Fox, A. M. (2001). Optical Properties of Solids, Oxford University Press.
7. Ignatovych, M., et al. (1999). "Spectral and Dosimetric Characteristics of Eu-Doped X-Ray Phosphors." Radiation Protection Dosimetry 84(1-4): 185-188.
8. J Bastow, T., et al. (1999). "Oxygen impurities in X-ray storage phosphors BaFBr and BaFCl investigated by 17O NMR." Journal of Physics: Condensed Matter 6(41): 8633.
9. Körner, M., et al. (2007). "Advances in Digital Radiography: Physical Principles and System Overview." RadioGraphics 27(3): 675-686.
10. Kubel, F., et al. (1996). "Synthesis and Structure of Ba12F19Cl5." Zeitschrift für anorganische und allgemeine Chemie 622(2): 343-347.
11. Leblans, P., et al. (2011). "Storage Phosphors for Medical Imaging." Materials (Basel, Switzerland) 4(6): 1034-1086.
12. Meng, X. and J. Zhou (2010). Photostimulated luminescence of BaFCl:Eu2+ in oxide glass ceramics.
13. Moy, J.-P. (2000). "Recent developments in X-ray imaging detectors." Nuclear Instruments and Methods in Physics Research Section A: Accelerators, Spectrometers, Detectors and Associated Equipment 442(1): 26-37.
14. Sauvage, M. (1974). "Refinement of the structures of SrFCl and BaFCl." Acta Crystallographica Section B 30(11): 2786-2787.
15. Secu, C. E., et al. (2007). "High temperature thermoluminescence of BaFCl:Eu2+ X-ray storage phosphor." physica status solidi c 4(3): 1016-1019.
16. Secu, M., et al. (2007). "Time-resolved luminescence spectroscopy of Eu 2+ in BaFCl:Eu 2+ X-ray storage phosphor." Journal of Optoelectronics and Advanced Materials 9(6): 1800-1802.
17. Secu, M., et al. (2000). "Preparation and optical properties of BaFCl:Eu2+ X-ray storage phosphor." Optical Materials 15(2): 115-122.
18. Stevels, A. L. N. and F. Pingault (1975). "BaFCl:Eu2+, a new phosphor for X-ray-intensifying screens." Philips Research Reports 30(5): 277-290
19. Yanagida, T. (2018). "Inorganic scintillating materials and scintillation detectors." Proceedings of the Japan Academy. Series B, Physical and biological sciences 94(2): 75-97.